

Confinement and pedestal structure in high performance scenarios in JET-ILW and comparison with JET-C

E. Stefanikova¹, L. Frassinetti¹, P. Lomas², I. Nunes³, M. Baruzzo⁴, F. Rimini², S. Saarelma², S. Wiesen⁵, M. Peterka^{6,7}, and JET contributors*

EUROfusion Consortium, JET, Culham Science Centre, Abingdon, OX14 3DB, UK

¹*Division of Fusion Plasma Physics, KTH Royal Institute of Technology, Stockholm SE*

²*CCFE, Culham Science Centre, Abingdon, OX14 3DB, UK; ³Centro de Fusao Nuclear, IST, Lisboa, Portugal;*

⁴*RFX, Corso Stati Uniti 4, Padova, Italy; ⁵Forschungszentrum Jülich GmbH, D-52425, Jülich, Germany;*

⁶*Institute of Plasma Physics AS CR, Prague, Czech Republic,*

⁷*Charles University in Prague, Faculty of Mathematics and Physics, Prague, Czech Republic*

* See the Appendix of F. Romanelli et al., *Proceedings of the 25th IAEA Fusion Energy Conference 2014, Saint Petersburg, Russia*

INTRODUCTION

High plasma current and field is one way to develop high performance scenarios with high thermal energy ($W_{th} > 10\text{MJ}$) and temperature ($T_e^{core} \approx 7\text{-}15\text{keV}$). Recently, JET-ILW has reached 4.0MA in the baseline scenarios with low triangularity in quasi stationary-conditions, avoiding W accumulation and controlling the divertor heat loads. The stored energy in JET-ILW tends to be lower than in JET-C [1]. This work studies the role of the pedestal in the confinement of JET-ILW baseline plasmas of a current scan and discusses the differences with the JET-C. The dataset used has I_p in the range 2-4.5MA, $P_{NBI} \approx 4\text{-}26\text{MW}$, gas level $\Gamma_{D2} \approx 0\text{-}10 \cdot 10^{22} \text{ e/s}$.

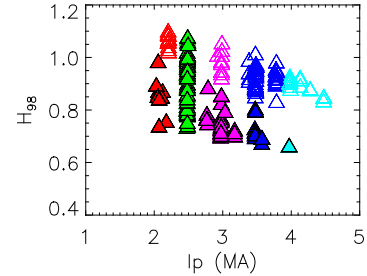


Figure 1. Range of H_{98} covered by JET-C (open symbols) and JET-ILW (full symbols) shots for different currents.

GLOBAL CONFINEMENT

The confinement enhancement factor covered by the analysed shots is $H_{98} \approx 0.6\text{-}1.1$, figure 1. For plasma current higher than 2.5MA, JET-ILW tends to have lower H_{98} than JET-C. For lower currents, JET-ILW can reach H_{98} comparable to JET-C.

Figure 2(a) shows the total stored thermal energy W_{th} versus the plasma current. An increase of W_{th} in both JET-C and JET-ILW with I_p is observed [1]. However, the increase is stronger in JET-C at high I_p . The stored energy in JET-ILW tends to be lower than in JET-C up to 20% for high I_p . Comparable W_{th} is obtained only for $I_p \leq 2.5\text{MA}$. The present JET-ILW dataset at high

I_p tends to have higher radiation from the bulk plasma but the lower W_{th} cannot be ascribed to a lower power through the separatrix. Figure 2(b) shows W_{th} versus $P_{sep} = P_{in} - dW_{th}/dt - P_{rad,bulk}$. At high current [light and dark blue color in the figure 2(b)] the stored energy in JET-ILW is lower than in JET-C, with P_{sep} in the range 15-25MW. The lower W_{th} in JET-ILW is related to a reduction in both the core W_{th} and in the pedestal W_{th} , as shown in figures 2(c) and 2(d) respectively.

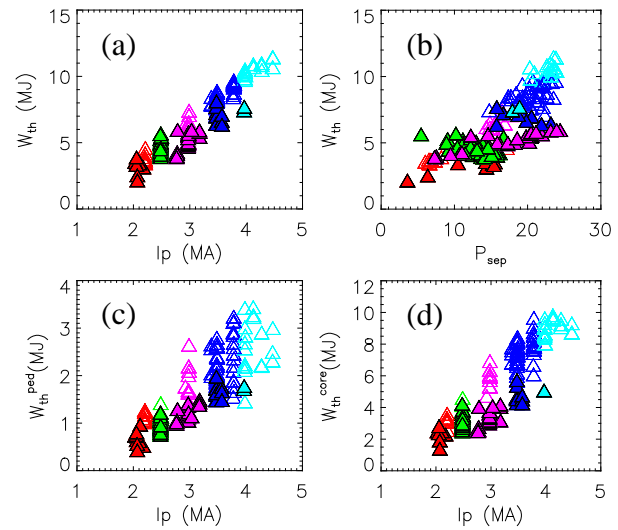


Figure 2. (a) Scaling of the total stored thermal energy with I_p ; (b) total stored thermal energy versus power through the separatrix; (c) core energy vs I_p ; (d) pedestal energy vs I_p . Open symbols – JET-C, full symbols – JET-ILW.

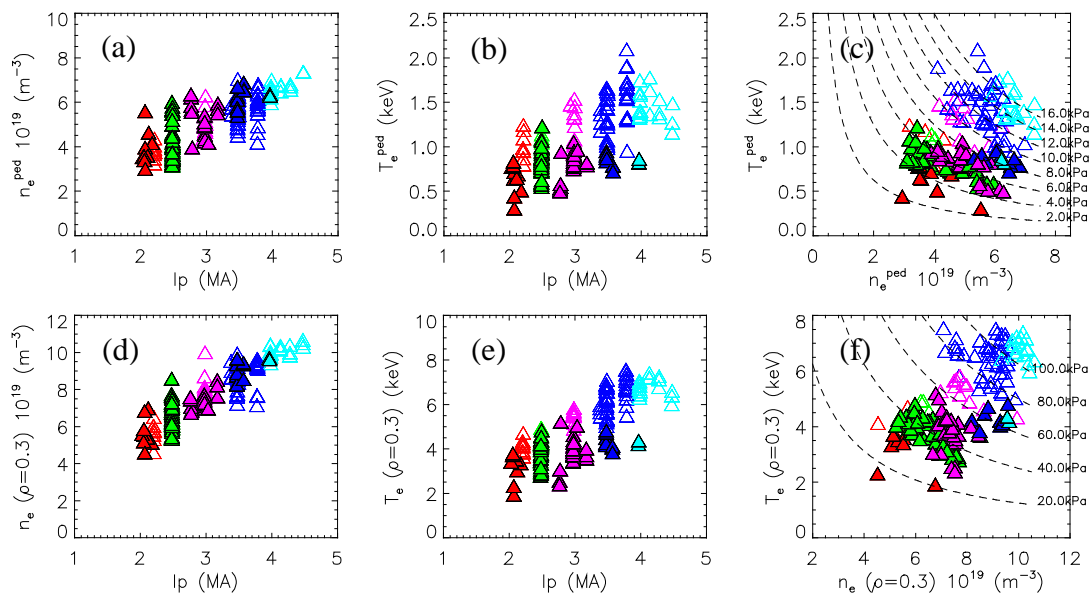


Figure 3. (a) Scaling of the pedestal density with current; (b) scaling of the pedestal temperature with current; (c) pedestal temperature vs pedestal density; (d) scaling of the core density with current; (e) scaling of the core temperature with current; (f) core temperature vs core density. Dashed lines indicate constant pressure. Open symbols – JET-C, full symbols – JET-ILW.

CORE AND PEDESTAL ELECTRON DENSITY AND TEMPERATURE

Figures 3(a) and 3(b) illustrate the scaling of pedestal density (n_e^{ped}) and temperature (T_e^{ped}) with I_p . In JET-C, both n_e^{ped} and T_e^{ped} increase with I_p . In JET-ILW, n_e^{ped} increases with I_p , and a good overlap with JET-C is observed. Instead, T_e^{ped} increases only until $I_p \approx 2.5$ MA. For $I_p > 2.5$ MA, T_e^{ped} is relatively constant, as already observed in [1]. Therefore, the low W_{th}^{ped} in JET-ILW is mainly due to a low T_e^{ped} . The difference in behaviour with I_p might be related to

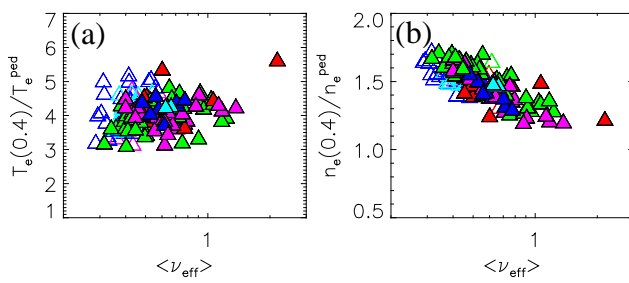


Figure 4. (a) T_e peaking vs ν_{eff} ; (b) n_e peaking as a function of ν_{eff} . Open symbols – JET-C, full symbols – JET-ILW. Colors correspond to levels of I_p .

the larger gas fuelling used in JET-ILW in order to control W accumulation [1]. The pedestal pressure (P_e^{ped}) in JET-ILW at high I_p does not reach values comparable to JET-C, figure 3(c). In the core, figures 3(d), 3(e) and 3(f), a similar behaviour to the pedestal is observed.

Figure 4 shows the dependence of profile peaking with the effective collisionality (ν_{eff}). Figure 4(a) shows that T_e peaking has a weak or no trend with ν_{eff} . Therefore a low T_e^{ped} is related to a low T_e^{core} due to the T_e profile stiffness. Figure 4(b) follows a decreasing trend of n_e peaking with ν_{eff} in agreement with [2]. JET-C and JET-ILW show the same trend of the peaking versus ν_{eff} . But, due to lower T_e at high current, JET-ILW tends to have higher ν_{eff} and therefore lower n_e peaking than JET-C. This further reduces the core contribution to the JET-ILW W_{th} .

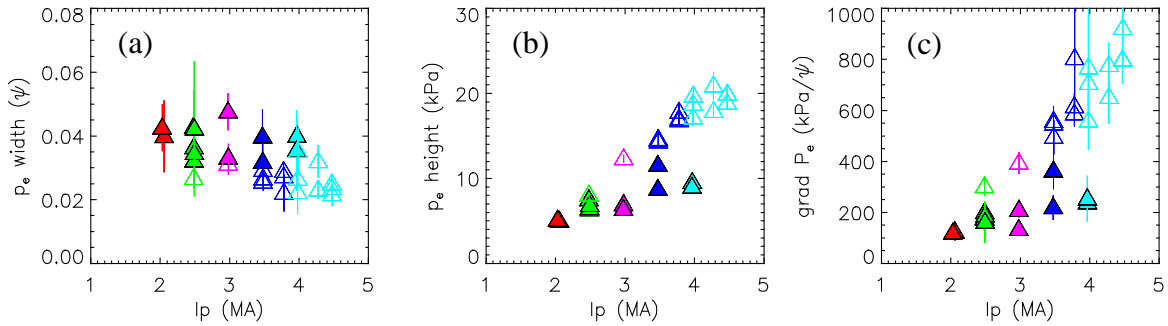


Figure 5. (a) p_e pedestal widths vs I_p ; (b) p_e pedestal heights vs I_p ; (c) grad p_e vs I_p . Open symbols – JET-C, full symbols – JET-ILW.

PEDESTAL WIDTH AND PEDESTAL GRADIENT

The pedestal width analysis has been performed at each I_p level for the shots with the highest H_{98} , both in JET-C and JET-ILW. Figure 5(a) shows pedestal p_e widths versus I_p . No clear trend with I_p is observed, but JET-C tends to have a lower pedestal width than JET-ILW. This might be related to the higher gas level used in JET-ILW [3]. Figure 5(b) shows the pedestal p_e versus I_p and figure 5(c) shows the correlation of the pedestal pressure gradient with I_p . A significant reduction, by a factor 2 or higher, for JET-ILW is observed.

STABILITY ANALYSIS

The stability analysis has been performed using the MISHKA and ELITE codes for the shot with the best confinement at each current level, in both JET-ILW and JET-C. The JET-C shots

are near or slightly beyond the stability boundary at each current level. Figure 6(a) and 6(b) show the stability diagram at $I_p = 2.5\text{MA}$ and $I_p = 4\text{MA}$ for JET-C. The JET-ILW shots are not far from the stability boundary only at low current ($I_p < 2.5\text{MA}$), while at high current JET-ILW is deep in the stable region, far from the boundary. Figure 6(c) and 6(d) show the stability diagram at $I_p = 2.5\text{MA}$ and $I_p = 4\text{MA}$ for JET-ILW. This is consistent with the fact that JET-ILW at high current has not reached performances comparable to the JET-C.

CONSLUSIONS

From the results above it can be concluded that low performance in JET-ILW (compared to JET-C) at high currents is due to a reduction in both core and pedestal stored energy and this is caused by a reduction of the T_e . Low T_e^{ped} produces low T_e^{core} due to T_e profile stiffness. Moreover, the low n_e peaking also reduces the contribution to W_{th}^{core} . Pedestal p_e widths from the selected subset of shots do not follow any obvious trend with I_p . But JET-ILW reaches comparable or larger pedestal widths than JET-C. Also the pressure gradient at the pedestal is strongly reduced in JET-ILW with high I_p . This is in accordance with stability analysis from the MISHKA code which showed that at high I_p JET-ILW is far from the stability boundary.

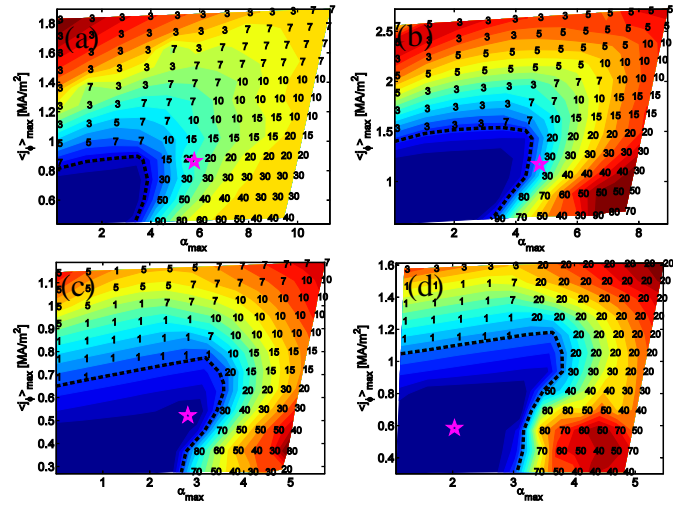


Figure 6. Stability diagram at (a) $I_p = 2.5\text{MA}$, JET-C, (b) $I_p = 4\text{MA}$, JET-ILW, (c) $I_p = 2.5\text{MA}$, JET-ILW, (d) $I_p = 4\text{MA}$, JET-ILW.

ACKNOWLEDGEMENTS

This work has been carried out within the framework of the EUROfusion Consortium and has received funding from the Euratom research and training programme 2014-2018 under grant agreement No 633053. The views and opinions expressed herein do not necessarily reflect those of the European Commission.

REFERENCES

- [1] I Nunes et al., EX/9-2 Proceedings of the 25th IAEA FEC 2014, Saint Petersburg, Russia
- [2] M. Beurskens et al., Nucl. Fusion **54**, 043001 (2014)
- [3] M. Leyland, et al., Nucl. Fusion **53**, 083028 (2013)